THE ASTROPHYSICAL JOURNAL, 413:L1–L5, 1993 August 10

A DEGREE SCALE ANISOTROPY MEASUREMENT OF THE COSMIC MICROWAVE BACKGROUND NEAR THE STAR GAMMA URSAE MINORIS

J. O. GUNDERSEN,[1,3] A. C. CLAPP,[2,3] M. DEVLIN,[2,3] W. HOLMES,[2,3] M. L. FISCHER,[2,3]
P. R. MEINHOLD,[1,3] A. E. LANGE,[2,3] P. M. LUBIN,[1,3]
P. L. RICHARDS,[2,3] AND G. F. SMOOT[3,4]
Received 1993 March 1; accepted 1993 May 18

ABSTRACT

Results from a search for anisotropy in the cosmic microwave background (CMB) are presented from the third flight of the Millimeter-wave Anisotropy eXperiment. Observations were made at 6, 9, and 12 cm^{-1} with a 0.°5 FWHM beam and a 1.°3 sinusoidal chop. The CMB observation occurred over 1.37 hours and covered a 6.24 deg^2 area of the sky where very little foreground emission is expected. Significant correlated structure is observed at 6 and 9 cm^{-1}. At 12 cm^{-1} we place an upper limit on the structure. The relative amplitudes at 6, 9, and 12 cm^{-1} are consistent with a CMB spectrum. The spectrum of the structure is inconsistent with thermal emission from known forms of interstellar dust. Synchrotron and free-free emission would both require unusually flat spectral indices at cm wavelengths in order to account for the amplitude of the observed structure. Although known systematic errors are not expected to contribute significantly to any of the three optical channels, excess sidelobe contamination cannot be definitively ruled out. If all the structure is attributed to CMB anisotropy, a value of the weighted rms of the 6 and 9 cm^{-1} channels of $\Delta T_{rms}/T_{CMB} = 4.7 \pm 0.8 \times 10^{-5}$ ($\pm 1\ \sigma$) was measured. If the CMB anisotropy is assumed to have a Gaussian autocorrelation function with a coherence angle of 25′, then the most probable value is $\Delta T/T_{CMB} = 4.2^{+1.7}_{-1.1} \times 10^{-5}$, where the $\pm$ refers to the 95% confidence limits. These values are similar to a measurement made in the same region of the sky on a previous flight; however, this lower limit is larger than the upper limit that was obtained in a different region of the sky during the same flight.

Subject headings: cosmic microwave background — cosmology: observations

1. INTRODUCTION

Measurements of the anisotropy of the cosmic microwave background (CMB) provide an effective method for testing and constraining models of cosmic structure formation. At small angular scales (< 10′) these measurements provide constraints on scenarios of galaxy formation. To date, only upper limits have been established on the anisotropy of the CMB at these small angular scales (Readhead et al. 1989). On large angular scales (> 5°), anisotropy measurements probe causally disconnected regions of the sky and provide critical information on the primordial gravitational potential fluctuations. The *Cosmic Background Explorer* (*COBE*) satellite has detected anisotropy at these large angular scales (Smoot et al. 1992). Anisotropy measurements on medium angular scales constrain scenarios of large-scale structure formation and the values of certain global parameters in cosmic evolution models (Bond et al. 1991 and Vittorio et al. 1991). Over the past 4 years, there has been a concerted effort to measure medium scale anisotropy (Meinhold & Lubin 1991; Fischer et al. 1992; Alsop et al 1992; Gaier et al. 1992). The results of a long CMB observation near Mu Pegasi during the third flight of the Millimeter-wave Anisotropy eXperiment (MAX) are reported in Devlin et al. (1993) and Meinhold et al. (1993a). We report here on the other CMB observation that occurred during the third flight of MAX.

2. INSTRUMENT

The instrument used to perform the observation reported here has been described in detail elsewhere (Fischer et al. 1992; Alsop et al. 1992; Meinhold et al. 1993b). The instrument consists of an off-axis Gregorian telescope and a bolometric photometer mounted on an attitude-controlled balloon platform. The off-axis Gregorian telescope consists of a 1 meter parabolic primary with a nutating elliptical secondary. The underfilled optics provide a 0.°5 full width, half-maximum (FWHM) beam that is sinusoidally modulated in azimuth at 6 Hz with a peak to peak throw of 1.°3 on the sky. The ^{3}He cooled bolometric photometer operates at 0.28 K with three optical channels centered at 6, 9, and 12 cm^{-1} (180, 270, and 360 GHz) with bandwidths given by $\delta\nu/\nu = 0.45, 0.35$, and 0.30. In order to convert antenna temperature measured in the 6, 9, and 12 cm^{-1} channels to 2.735 K thermodynamic temperature, one must multiply by 2.36, 5.70, and 21.3, respectively. A bolometer with a metal cover over the optical path (called the blank channel) is used as a check for systematic effects such as radio frequency interference (RFI).

3. OBSERVATION

The deep CMB observation reported here was made in a region near the star Gamma Ursae Minoris (GUM) $\alpha = 15^h20^m.7$, $\delta = 71°52'$ (Epoch 1991). The GUM region was chosen since significant structure was observed in this region during the second flight of MAX (Alsop et al. 1992) and because this region has low dust contrast as measured at 100

[1] Department of Physics, University of California, Santa Barbara, CA 93106.
[2] Department of Physics, University of California, Berkeley, CA 94720.
[3] NSF Center for Particle Astrophysics, University of California, Berkeley, CA 94720.
[4] Space Sciences Laboratory and Lawrence Berkeley Laboratory, Building 50-351, University of California, Berkeley, CA 94720

μm by *IRAS*. The complete GUM scan lasted for 1.37 hours between UT = 4.08 hours and UT = 5.45 hours, 1991 June 5. A calibration was performed from UT = 4.71 to UT = 4.84 hours using the membrane transfer standard described in Fischer et al. (1992). The scan pattern consisted of constant velocity scans in azimuth of $\pm 3.^{\circ}0$ on the sky while tracking GUM. Due to sky rotation, the observed region is shaped like a bow tie with right ascension ranging from $\alpha = 14^{h}52^{m}$ to $\alpha = 16^{h}8^{m}$ and declination ranging from $\delta = 71^{\circ}12'$ to $\delta = 72^{\circ}24'$ (Epoch 1991).

4. DATA REDUCTION

Transients due to cosmic rays were removed using an algorithm described in Alsop et al. (1992). This excluded 5% to 10% of the data. The detector output was demodulated using the sinusoidal reference from the nutating secondary to produce antenna temperature differences, ΔT_A, on the sky. Data sets were produced that are in phase with the optical signal (optical phase) and 90° out of phase. The phase synchronous demodulation produced a value for each nutation cycle (every 180 ms) except when a cosmic ray was detected. In addition, there were very brief, aperiodic RFI transients which were strongly correlated in time between the optical channels and the blank channel. Data in all optical channels were removed at a given time if there was a transient in the blank channel *and* any of the optical channels. This criterion eliminated 12% of the data and reduced the 1 σ error bars in the binned data for the 6 cm^{-1} and blank channel by 30% to 40%. The error bars for the 9 and 12 cm^{-1} channels were only slightly reduced. The short-term noise averaged over a 20 second time period gives effective sensitivities of 533, 731, and 1940 $\mu K\sqrt{sec}$ in CMB thermodynamic units in the 6, 9, and 12 cm^{-1} channels, respectively. These results are consistent with measurements made before the flight. Neither the amplitude nor the morphology in any optical channel was significantly affected by the RFI removal. Chi-square tests show that the RFI did not induce structure since there is *no* statistically significant structure in either phase of the blank channel or in the 90° phase of the optical channels. In addition, Table 1 shows that the spectrum of the removed RFI data is unlike the observed spectrum.

5. ANALYSIS

The first step in the analysis is to remove an offset from each full scan in azimuth. The average of the measured offsets in antenna temperature were 2.26, 1.39, and 2.98 mK in the 6, 9, and 12 cm^{-1} channels. The blank channel had an average offset of 0.02 mK when referenced to the 9 cm^{-1} channel. None of the optical channels' offsets varied by more than a few percent over the complete scan. The offset removal does not affect the scan-correlated structure. The means, variances and 1 σ error bars of the antenna temperature differences were calculated for 39 equal area pixels, each of which is 24′ square. The means and 1 σ error bars do not depend significantly on whether the offset was removed. Figure 1 shows 16 of the 39 pixels taken from a slice at $\delta = 72^{\circ}24'$. A map showing all pixel positions, means, and error bars is available from the authors. The essential features of the data are apparent in Figure 1. First, there is statistically significant structure in the 6, 9, and 12 cm^{-1} channels. The rms values of ΔT_A are 48 ± 10, 26 ± 6, and 11 ± 3 μK for the 6, 9, and 12 cm^{-1} channels, respectively. These rms values of ΔT_A are the square root of the difference between the variance of the 39 pixel means and the variance due to detector noise. The error on each rms includes a statistical error and a $\pm 10\%$ estimate for the systematic error in the absolute calibration. The values of the reduced χ^2 for 38 degrees of freedom are 4.02, 3.93, and 2.01, respectively. Second, Figure 1 shows a large correlated component in the 6 and 9 cm^{-1} channels which is much smaller in the 12 cm^{-1} channel. Third and last, the amplitude of the structure as measured in antenna temperature decreases with increasing frequency.

In order to test the hypothesis that the structure in all three channels is correlated, a best-fit model was determined by minimizing

$$\chi_R^2 = \sum_{j=1}^{3} \sum_{i=1}^{39} (x_{ij} - a_j y_i)^2 / \sigma_{ij}^2 , \qquad (1)$$

where x_{ij} and σ_{ij} are the measured means and sigmas of the 39 pixels, y_i is the best-fit sky model, and and a_j are the best-fit model scale factors. The probability of exceeding the residual χ_R^2 was less than 0.01, and this hypothesis was rejected. Instead, the hypothesis that the structure at 6 and 9 cm^{-1} is correlated was tested. As shown in Table 1, this has a much higher probability of exceeding the residual χ^2. The best fit ratio, which is the ratio of the respectives a's in equation 1, is compared in Table 1 with the expected channel ratios for the CMB and a variety of common foregrounds. This procedure is repeated for the 12/6 and 12/9 ratios; however, since the 12 cm^{-1} structure is not significantly correlated with 6 and 9 cm^{-1} structure, the 9/6 ratio provides the most useful constraint on spectra which

TABLE 1

SPECTRAL CONSTRAINTS ON THE OBSERVED SIGNALS

Channel Ratio (1)	Best-Fit Ratios of Antenna Temperature (2)	Probability of Exceeding Residual χ_R^2 (3)	CMB Ratio (4)	Synchrotron Ratio for $\Delta T_A \propto \nu^{-2.7}$ (5)	Free-Free Ratio for $\Delta T_A \propto \nu^{-2.1}$ (6)	Cold Dust Ratio (7)	Warm Dust Ratio (8)	Ratio of Removed RFI Points (9)
9/6.....	0.53 ± 0.11[a]	0.19	0.41	0.31	0.41	1.55	1.69	0.04 ± 0.03
12/6.....	$<0.19 + 0.08$[b]	0.02	0.11	0.13	0.20	1.72	2.60	0.02 ± 0.03
12/9.....	$<0.36 + 0.13$[b]	0.02	0.27	0.40	0.48	1.11	1.54	0.09 ± 0.04

[a] Best-fit ratio ± 1 σ error.

[b] Upper limits on the best-fit ratios $+1$ σ error.

NOTES.—Explanation of selected columns: (col. [3]) The probability of exceeding residual χ_R^2 is a measure of how well a best-fit channel ratio describes the amplitude scaling between two channels for 37 degrees of freedom; (cols. [4]–[8]) the expected channel ratios were determined by integrating the respective spectra over each of the bandpasses; (cols. [7]–[8]) the dust spectra assume that the brightness is given by $I(\nu, T) \propto \nu^n B(\nu, T)$, where $B(\nu, T)$ is the Planck blackbody brightness; (col. [7]) cold dust assumes $T = 4.77$ K and $n = 2$ (Wright et al. 1991); (col. [8]) warm dust assumes $T = 20$ K and $n = 1.4$; (cols. [2] and [9]) the errors on the ratios include a statistical error and a $\pm 10\%$ estimate for the systematic error in the relative calibration.

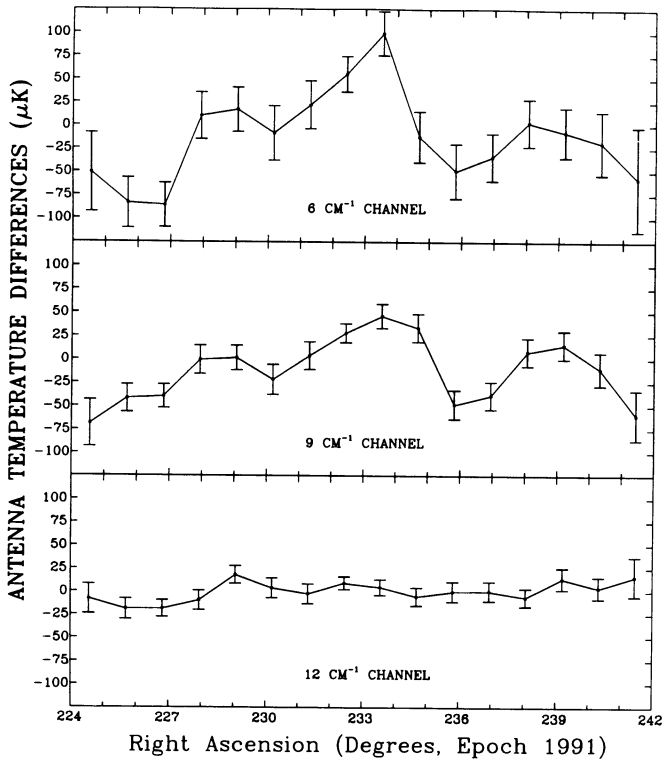

FIG. 1.—Antenna temperature differences ($\pm 1\ \sigma$) for 16 of the 39 contiguous 24′ × 24′ equal area pixels for the 6, 9, and 12 cm^{-1} channels at $\delta = 72°.4$.

fall with frequency. The absence of correlated structure at 12 cm^{-1} places stringent limits on spectra which rise with frequency.

6. DISCUSSION

In the following, a discussion of potential sources of confusion is presented, and the observed structure is characterized and compared to other anisotropy measurements.

MAX is potentially susceptible to sidelobe contamination from the Sun, Moon, Earth, the balloon, and the Galactic plane. The unchopped sidelobe response has been measured to be ≥ 65 dB below the mainlobe response at angles from 12° to 45° in elevation from boresight. No comparably deep measurements have been made of the chopped sidelobe response in azimuth. During the GUM measurement the Sun and Moon were both below the horizon. The elevation angle varied from 48°.5 to 50° as the telescope tracked GUM through transit. The most striking evidence that the structure is not due to sidelobes comes from the Mu Pegasi scan (Meinhold et al. 1993a) which tracked in elevation from 36° to 45° during the first half of the scan and from 46° to 55° during the second half of the scan. Any sidelobe contamination from the Earth is expected to be larger in the first half of the Mu Pegasi scan than in the GUM scan. Also, any sidelobe contamination from the balloon would be larger in the second half of the Mu Pegasi scan than in the GUM scan. The 95% confidence level upper limits to the Gaussian autocorrelation function (GACF) at 25′ for the Mu Pegasi scan (after subtracting structure identified as dust emission) are $\Delta T/T_{CMB} = 2.6 \times 10^{-5}$ and 2.9×10^{-5} for the first and second halves, respectively. These limits on the sidelobe contamination are considerably less than the structure in the GUM scan. During the GUM scan, the closest approach of the Galactic plane was 36° at $l^{II} = 105°$. For the Mu Pegasi scan, the relative orientation of the scan with respect to the Galactic plane was similar to the GUM scan, and the galactic plane was closer than 36°. Yet, based on the complete Mu Pegasi scan, an upper limit of $\Delta T/T_{CMB} = 2.5 \times 10^{-5}$ can be placed on any sidelobe contribution from the Galactic plane. Although these arguments cannot be used to rule out sidelobe contamination, they suggest that the structure in the GUM scan is not dominated by sidelobe contamination.

The falling spectrum of the observed structure indicates that it is not due to the atmosphere. When the spectrum of the atmosphere is integrated over the bandpasses, the contribution to the antenna temperature in the 12 cm^{-1} channel is 2 to 10 times larger than the contribution in the 6 or 9 cm^{-1} channels, depending on whether the contamination is due to water, ozone, or oxygen. The comparatively small signal in the 12 cm^{-1} band is inconsistent with atmospheric contamination as a source of the observed structure at 6 and 9 cm^{-1}.

Potential Galactic/extragalactic sources of confusion include interstellar dust emission, synchrotron radiation, free-free emission, molecular line emission from CO and the Sunyaev-Zel'dovich (SZ) effect. At 6, 9, and 12 cm^{-1} the predominant Galactic/extragalactic source of confusion is expected to be emission from interstellar dust. The falling spectrum of the observed structure is not consistent with dust emission (as shown in Table 1). In addition, based on an extrapolation from the *IRAS* 100 μm data, the differential dust emission in the GUM region is expected to be very low. The measurement was simulated on an *IRAS* 100 μm map with 1′.5 × 1′.5 pixels from the *IRAS* Sky Survey Atlas (Wheelock et al. 1991). The resulting morphology does not correlate with the observed morphology and the rms amplitude (using scalings from Meinhold et al. 1993a) is a factor of 3 below the measured structure at 12 cm^{-1}. The observed spectrum of the structure is also inconsistent with the SZ effect, which would produce anti-correlated structure at 6 and 9 cm^{-1}.

The rms differential antenna temperature due to diffuse synchrotron emission in the GUM region is not more than 2 K at 408 MHz as given in the 30′ × 30′ smoothed version of the Haslam et al. (1982) map. Assuming a scaling law $\Delta T_A \propto \nu^{\beta}$ for synchrotron emission with $\beta = -2.7$ implies an rms $\Delta T_A \leq 0.15$, 0.05, and 0.03 μK at 6, 9, and 12 cm^{-1}, respectively. These estimates are less than 1% of the observed structure. The largest gradient in the 408 MHz Haslam map in this region is due to the quasar 3C 309.1 which is a very well studied compact, steep spectrum (CSS) radio source. The estimated signal from 3C 309.1, based on measurements at 80 and 230 GHz by Steppe et al. (1988) and Kreysa (1992) is $\Delta T_A = 6.2$, 2.5, and 1.1 μK at 6, 9, and 12 cm^{-1}, respectively. This is less 10% of the observed structure in the position of the quasar. The statistical significance of the structure in the scan does not change if the pixels overlapping 3C 309.1 are removed, so our result is independent of the brightness of 3C 309.1. A compilation by Kuhr et al. (1981) (which is essentially complete out to 250 mJy at 2.7 GHz) lists other less bright radio sources in the GUM region that have been measured at 2.7, 5, and 10.7 GHz. Unless any of these source have flat or inverted spectra beyond 10.7 GHz, it is unlikely that they could contribute to the observed structure.

Free-free emission is the least well characterized of the potential Galactic contaminants. No small-scale Hα data are available for the GUM region. If we assume that the Hα background can be represented by the free-free brightness temperature, $T_{ff} \cong 1 \times 10^{-2} \nu_{GHz}^{-2.1} \csc |b^{II}|$ K, given by Reynolds

(1992), then background brightness temperatures of $T_{ff} = 0.3$, 0.12, and 0.07 μK can be estimated at 6, 9, and 12 cm^{-1}, respectively. The observations of diffuse Hα by Reynolds (1992) suggest that typical differential temperatures at the observed Galactic latitude and angular scale are roughly twice the background level, and that there may be a few bright, high latitude H II regions with differential brightness temperatures an order of magnitude larger than this. In this extreme case, the expected rms differential antenna temperatures due to free-free emission would be $\Delta T_A = 6$, 2.4, and 1.4 μK in the 6, 9, and 12 cm^{-1} bands, respectively. This is less than 10% of the observed structure. An alternative estimate is obtained from the conservative assumption that the entire 408 MHz rms (excluding the quasar) is due to free-free emission and extrapolating to our frequencies using $\Delta T_A \propto \nu^{-2.1}$. This estimate gives 10% of the measured rms. Although the relative millimeter-wave amplitudes of the structure are consistent with free-free emission, the two estimates of the free-free contribution to ΔT_A show that this is also an unlikely contaminant.

Sources of molecular line emission at our frequencies include the CO ($J = 1$–0) transition which is below the low frequency cutoff of the 6 cm^{-1} channel, the 2–1 transition which would contaminate both the 6 and 9 cm^{-1} channels, and the 3–2 transition which would only appear in the 12 cm^{-1} channel. Formations as large as several square degrees containing CO emission have been shown to exist at high Galactic latitudes with 2–1 intensities that peak as high as 7 K km s^{-1} (e.g., Magnani, Blitz, & Mundy 1985). Measurements of the 1–0 transition in the GUM region show that there is no emission above 1 K km s^{-1} (Wilson & Koch 1992; Thaddeus & Dame 1993). A 1 K km s^{-1} CO cloud filling a beam would cause approximately a 10 μK signal at 6 cm^{-1} and a 5–10 μK signal at 9 cm^{-1}.

Since all of the known possible foreground contaminants are considered unlikely and the spectrum of the structure is consistent with CMB anisotropy, the following discussion interprets the observed structure as CMB anisotropy. The size of this anisotropy is characterized, and the structure is compared to other measurements on various angular scales. One measure of structure is the weighted rms of the 6 and 9 cm^{-1} data which give $\Delta T_{rms}/T_{CMB} = 4.7 \pm 0.8 \times 10^{-5}$ ($\pm 1\ \sigma$). This rms is dependent on the spatial filter determined by the 0.°5 beam size, the 1.°3 sinusoidal chop, and the scan strategy. A specific model is needed in order to compare these measurements to data measured at larger angular scales. Standard cold dark matter (CDM) models normalized to the rms amplitude of the anisotropy measured by *COBE* at $\theta > 10°$ predict an rms amplitude for our window function of approximately $\Delta T_{rms}/T_{CMB} = 2$–3 $\times 10^{-5}$ (Bond 1992; Gorski 1993). A detailed comparison of our results with theoretical models is left for future publications.

Other measures of structure include the most probable amplitude and the 95% confidence level upper and lower limits to a particular autocorrelation function. Due to sky rotation and the smooth scan strategy, the expression for the expected sky variance, as given in equation (4) of Vittorio et al. (1991), must be modified. The data set is binned into 11 different rotation angles with four complete scans per rotation angle. Every possible product of temperature differences is enumerated in the theoretical covariance matrix $\boldsymbol{M}$, given as

$$\boldsymbol{M}_{i*(|k-k'|+1),i'*(|k-k'|+1)} = \langle \Delta T_{ik} \Delta T_{i'k'} \rangle + \sigma_{ik}^2 , \qquad (2)$$

where the unprimed and primed indices refer to any two temperature differences, respectively, and σ_{ik} is the measured 1 σ error for $i = 1$ to 15 scan angles and $k = 1$ to 11 rotation angles. The first term in the above expression can be written in terms of the correlation functions (analogous to eq. [6] of Readhead et al. 1989) as

$$\langle \Delta T_{ik} \Delta T_{i'k'} \rangle = C(\varphi_0, \varphi_1) - C(\varphi_0, \varphi_2) - C(\varphi_0, \varphi_3) + C(\varphi_0, \varphi_4) , \qquad (3)$$

where $\varphi_1 = |\boldsymbol{x}_{ik}^+ - \boldsymbol{x}_{i'k'}^+|$, $\varphi_2 = |\boldsymbol{x}_{ik}^+ - \boldsymbol{x}_{i'k'}^-|$, $\varphi_3 = |\boldsymbol{x}_{ik}^- - \boldsymbol{x}_{i'k'}^+|$, $\varphi_4 = |\boldsymbol{x}_{ik}^- - \boldsymbol{x}_{i'k'}^-|$, φ_0 is the beam dispersion ($= 13'$) with the "+" and "−" labeling the respective chop positions, and $\boldsymbol{x}$ is the angular distance vector. The sky is modeled as having a GACF as given in equation (12) of Readhead et al. (1989). A Bayesian method assuming a uniform prior likelihood distribution has been used to calculate a most probable amplitude of $\Delta T/T_{CMB} = 4.2^{+1.7}_{-1.1} \times 10^{-5}$, where the $\pm$ refers to the 95% confidence level upper and lower limits to the GACF at the most sensitive angular scale of 25′. The size of the observed structure is similar to that observed in the second flight of MAX which measured a most probable amplitude of $4.5^{+5.7}_{-2.6} \times 10^{-5}$ (Alsop et al. 1992). A direct comparison of the morphology of this data set with the results from the second flight is impossible since the scans only overlapped in a 0.5 deg^2 area. In the Mu Pegasi scan (Meinhold et al. 1993a), a 95% confidence level upper limit of 2.4×10^{-5} is set for fluctuations at an angular scale of 25′. The lower limit obtained from the GUM scan is larger than the upper limit obtained from the Mu Pegasi scan. Therefore, if all the structure measured in the GUM scan is CMB anisotropy, the hypothesis that CMB anisotropy is Gaussian distributed is ruled out at the 3 σ level.

7. CONCLUSION

We have presented new results from a search for CMB anisotropy with high sensitivity at angular scales near 1 degree. Significant structure is detected at an rms level $\Delta T_{rms}/T_{CMB} = 4.7 \pm 0.8 \times 10^{-5}$ ($\pm 1\ \sigma$). Based on the Mu Pegasi scan, sidelobe contamination from the Earth, balloon, and the Galaxy is expected to be considerably less than the observed structure. Atmospheric and RFI contamination are improbable due to the lack of structure in the 12 cm^{-1} and blank channels, respectively. The data rule out Galactic dust emission via the spectrum, morphology and amplitude of the structure. Synchrotron and free-free emission are considered unlikely contaminants from estimates of their intensity based on low-frequency maps. The relative amplitude of the structure at 6, 9, and 12 cm^{-1} is consistent with CMB anisotropy. The amplitude of the structure is similar to a previous observation made in the same region. The structure is significantly larger than the 95% confidence level upper limits determined from measurements made during this flight near Mu Pegasi and other 95% confidence level upper limits made at similar angular scales by others in different regions of the sky.

This work was supported by the National Science Foundation through the Center for Particle Astrophysics (cooperative agreement AST-9120005), the National Aeronautics and Space Administration under grants NAGW-1062 and FD-NAGW-2121, the University of California, and previously California Space Institute. Thanks are due to Robert Wilson and Tim Koch (1992) and Patrick Thaddeus and Tom Dame (1993) for making CO measurements in the GUM region.

REFERENCES

Alsop, D. C., et al. 1992, ApJ, 317, 146
Bond, J. R. 1992, private communication
Bond, J. R., et al. 1991, Phys. Rev. Lett., 66, 2179
Devlin, M., et al. 1993, in Proc. NAS Colloq. Physical Cosmology (Irvine), in press
Fischer, M., et al. 1992, ApJ, 388, 242
Gaier, T., et al. 1992, 398, L1
Gorski, K. 1993, preprint
Haslam, C. G. T., et al. 1982, A&AS, 47, 1
Kreysa, E. 1992, private communication
Kuhr, H., et al. 1981, AJ, 86, 6
Magnani, L., Blitz, L., & Mundy, L. 1985, ApJ, 295, 402
Meinhold, P. R., & Lubin, P. M. 1991, ApJ, 370, L11
Meinhold, P. R., et al. 1993a, ApJ, 409, L1
———. 1993b, ApJ, 406, 12
Readhead, A. C. S., et al. 1989, ApJ, 346, 566
Reynolds, R. J. 1992, ApJ, 392, L35
Smoot, G. F., et al. 1992, ApJ, 396, L1
Steppe, H., et al. 1988, A&AS, 75, 317
Thaddeus, P., & Dame T. 1993, private communication
Vittorio, N., et al. 1991, ApJ, 372, L1
Wheelock, S., et al. 1991, *IRAS* Sky Survey Atlas
Wilson, R., & Koch, T. 1992, private communication
Wright, E. L., et al. 1991, ApJ, 381, 200